DIELECTRIC-COATED SPHERICALLY-TIPPED CONDUCTING CONE ANTENNA EXCITED IN THE UNSYMMETRIC HYBRID MODE AT MICROWAVE FREQUENCIES

R. CHATTERJEE AND T. S. VEDAVATHY

(Department of Electrical Communication Engineering, Indian Institute of Science, Bangalore 560012, India)

Received on May 16, 1975 and in revised form on August 25, 1975

ABSTRACT

An approximate theory has been derived for the radiated field and gain of the dielectric-coated spherically-tipped conducting cone antenna excited in the unsymmetric hybrid mode, assuming a given distribution of surface currents on the antenna. The calculated radiation patterns and gain of a large number of antennas of varying dimensions have been verified by experiment in the X-band. The measured input impedance of the antennas has been reported.

1. INTRODUCTION

In 1950, Schorr and Beck [1] studied the problem of electromagnetic radiation from a conducting conical horn. Significant contributions have been made by Felsen [2-6] to the problem of scattering of electromagnetic waves by conducting conical structures and also to the problem of radition from tapered surface wave antennas [7]. The radiation characteristics of a semi-infinite conducting cone antenna, as well as that of a finite cone has been studied by Adachi [8, 9], as review of the radiation characteristics of the conical structures has been given by Wait [10]. As far as the authors are aware of, there has been no work on dielectric-coated conducting cone-antennas till 1964. In 1964, Yeh [11] has introduced the use of Sommerfeld's complex-order wave functions in deriving theoretically the radiation characteristics of a dielectric-coated spherically-tipped semi-infinite conducting cone excited in the symmetric TM mode, but there is no experimental verification. Chatterjee [12] has made a rigorous theoretical analysis of the electromagnetic boundary-value problem of the dielectric-coated spherically-tipped semi-infinite conducting cone, and has shown that symmetric TE, symmetric TM and symmetric and unsymmetric hybrid modes can be supported by such a structure, but that unsymmetric TE or TM modes cannot be supported. Subsequently the radiation characteristics of finite length dielectric-coated spherically-tipped conducting cone antennas have been studied theoretically by an approximate method by the authors and verified experimentally [13, 14].

In this paper an approximate theory for the radiated field and gain of the finite length dielectric-coated spherically-tipped conducting antenna excited in the unsymmetric hybrid mode has been derived, assuming a given distribution of surface currents on the antenna. The calculated radiation patterns and gain of a large number of antennas of varying dimensions as well as the assumed surface current distribution have been verified by experiment. The measured input impedance of the antennas has also been reported.

2. GEOMETRY OF THE STRUCTURE

Figure 1 shows the geometry of the structure. The antenna consists of a dielectric-coated spherically-tipped conducting cone $A'AOBB'$. This

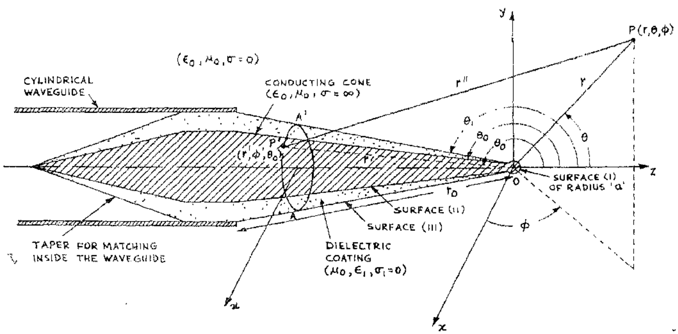

FIG. 1

antenna is excited by a mode transformer which is a TE_{11} mode circular cylindrical waveguide. The TE_{11} mode in the circular metal waveguide is transformed into the first unsymmetric hybrid mode in the dielectric-coated spherically-tipped conducting cone. The spherical polar coordinates of any point on the structure are designated (r', θ', ϕ'), while those of a distant point are designated (r, θ, ϕ).

3. Estimate of the Surface Currents on the Antenna

The determination of the radiated field requires a knowledge of the field components and hence the surface currents on the surface of the antenna. The field distributions on the surface of the antenna are determined by utilizing the field components of the TE_{11} mode in the circular cylindrical conducting waveguide which acts as a launcher and also from a knowledge of the near field variations along the coordinate directions r', θ', ϕ' obtained by measurements with the help of appropriate field probes.

The components of the electromagnetic field inside a hollow metal circular waveguide progpagating the dominant TE_{11} mode are:

$$H_z = C_1 J_1 (h\rho) \cos\phi \exp j(\omega t - \bar{\beta} z) \tag{1}$$

$$H_\rho = \frac{-j\bar{\beta}C_1}{h} J_1'(h\rho) \cos\phi \exp j(\omega t - \bar{\beta} z) \tag{2}$$

$$H_{\phi'} = \frac{j\bar{\beta}C_1}{h^2\rho} J_1(h\rho) \sin\phi \exp j(\omega t - \bar{\beta} z) \tag{3}$$

$$E_{\rho'} = \frac{\omega\mu_0}{\bar{\beta}} H_{\phi'} \tag{4}$$

$$E_{\phi'} = \frac{-\omega\mu_0}{\bar{\beta}} H_\rho \tag{5}$$

$$E_z = 0 \tag{6}$$

where

$$h = \frac{1\cdot 84}{a}, \text{ '}a\text{' being the radius of the cylinder, and}$$

$$\bar{\beta} = \sqrt{\omega^2 \mu_0 \epsilon_0 - h^2}. \tag{7}$$

The measurements of the near field of the antenna show that all the field components vary as $\cos\phi$ or $\sin\phi$ (Fig. 2). Hence thefield components inside the cylindrical waveguide as given by equations (1) to (6) may be approximately assumed to be transformed to $H_{r'}$, $H_{\theta'}$, $H_{\phi'}$, $E_{r'}$ $E_{\theta'}$ and $E_{\phi'}$ in the dielectric coated spherically-tipped conducting cone according to the following transformation:

$$H_{r'} = H_z \cos\theta + H_\rho \sin\theta \tag{8}$$

$$H_{\theta'} = -H_z \sin\theta + H_\rho \cos\theta \tag{9}$$

$$H_{\phi'} = H_{\phi'} \tag{10}$$

and similar equations for $E_{r'}$, $E_{\theta'}$, and $E_{\phi'}$.

The tangential electric field components on the inner surface of the conducting cylindrical waveguide is zero. Hence it is assumed that the tangential electric field components on the outer surface (iii) of the dielectric coating (Fig. 1) are negligible compared to the tangential magnetic field components. The tangential electric field components on the spherical metal tip (i) are zero. Hence it is assumed that only the surface electric currents due to the tangential magnetic fields on the surface of the antenna contribute to the radiated field at a distant point. The spherical tip (i) being very small compared to the cone, the contribution of surface electric currents on it to the radiated field are neglected in comparison with the contribution of the surface electric currents on surface (iii) of the dielectric-coated metal cone. Thus

only $\quad \vec{u}_{\phi'} J_{\phi'} = - \vec{n} \times \vec{u}_{r'} H_{r'}$

and $\quad \vec{u}_{r'} J_{r'} = - \vec{n} \times \vec{u}_{\phi'} H_{\phi'}$

are considered to be the predominant components of surface electric current on the surface (iii) which contribute to the radiated field.

From equations (1) to (10), $H_{r'} \alpha \cos \phi'$ and $H_{\phi'} \alpha \sin \phi'$, and thus $| H_{r'} |$ and hence $| J_{\phi'} |$ may be taken as $\alpha\, Re \exp (j\phi')$, and $| H_{\phi'} |$ and hence $| J_{r'} |$ may be taken as $\alpha I_m \exp (j\phi')$.

The following assumption for the variation of the field components $H_{r'}$ and $H_{\phi'}$ with the space coordinates and time and hence for the surface currents $J_{\phi'}$ and $J_{r'}$ respectively can be made;

$$J_{\phi'} = - H_{r'} = \frac{K_1 \exp (j\omega t)}{k_2 r'} [\exp (jk_2 r') + R \exp (- jk_2 r')]\, Re \exp (j\phi') \tag{11}$$

$$J_{r'} = - H_{\phi'} = \frac{K_2 \exp (j\omega t)}{k_2 r'} [\exp (jk_2 r') + R \exp (- jk_2 r')]\, Im \exp (j\phi') \tag{12}$$

where the constants K_1 and K_2 are determined from equations (8) and (9), knowing the field components H_ρ, $H_{\phi'}$, Hz inside the cylindrical conducting waveguide which excites the dielectric-coated spherically-tipped conducting cone.

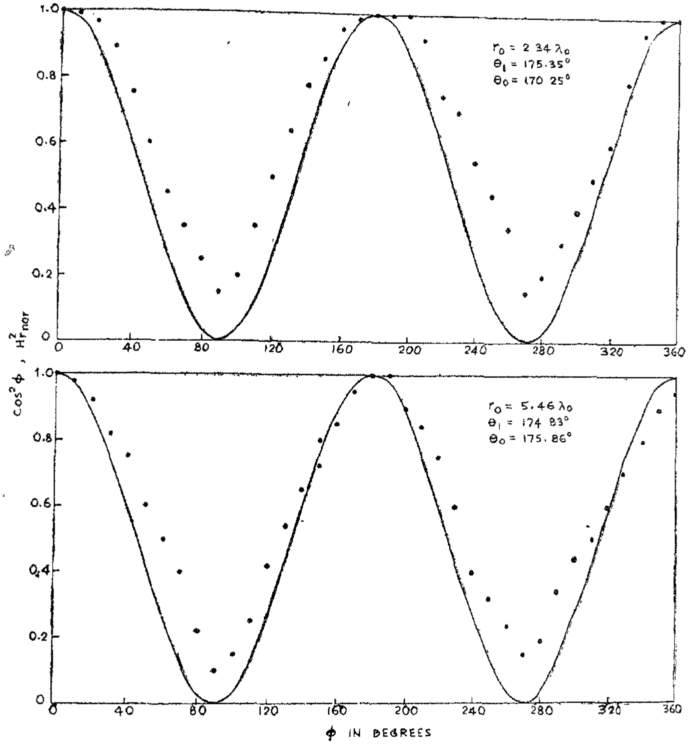

Fig. 2 Variation of power (H_r^2) with ϕ in the vicinity of the aerial
—— $\cos^2\phi$ (Theoretical), • • • H_r^2 Experimental

The nature of variation of the field components as given by equations 11) and (12) are justified by experimental results (Figs. 3 and 4).

$k_2 = 2\pi/\lambda g$, where λ_g is the measured guide wavelength in the dielectric-coated spherically-tipped conducting cone and is twice the average distance

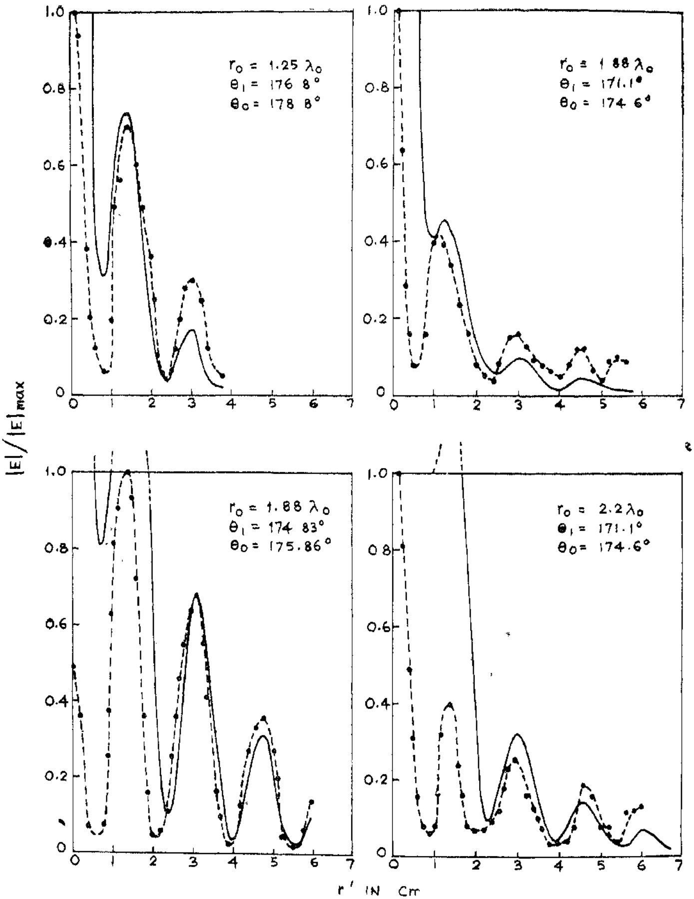

FIG. 3. Standing wave pattern along the surface of the aerial.
—— Calculated, —●—●— Experimental.

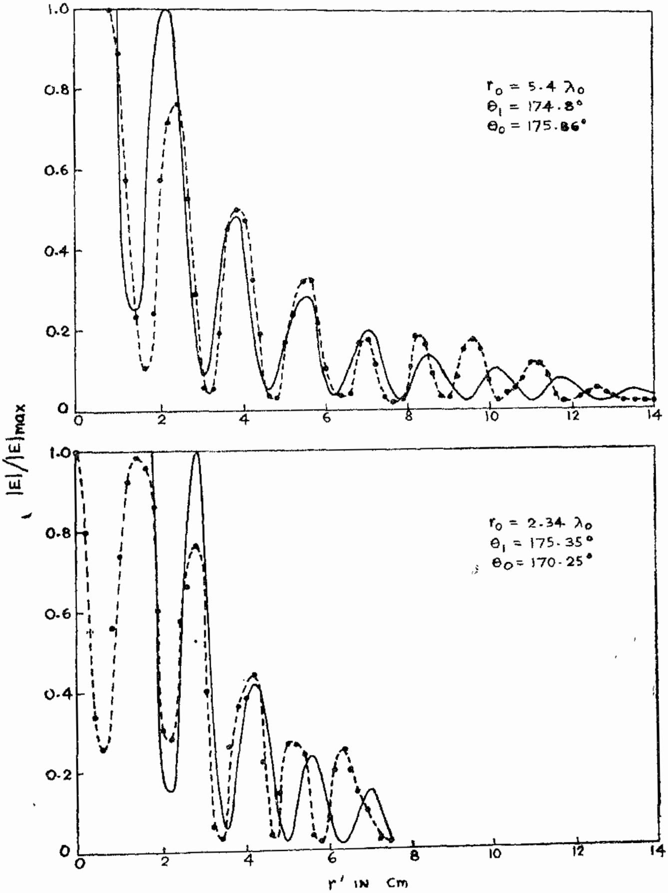

FIG. 4. Standing wave pattern along the surface of the aerial.
—— Calculated, —●—●— Experimental.

between maxima or minima of the standing-wave pattern on the surface of the struture. R is the measured reflection coefficient in the structure and it is evaluated by using the fomula

$$R = \frac{VSWR - 1}{VSWR + 1}$$

where $VSWR$ is the average $VSWR$ as obained from the curves shown in Figs. 3 and 4. Equations (11) and (12) show that $J_{\phi'}$ and $J_{r'}$ both consist of two travelling spherical waves one in the positive r' direction and the other in the negative r' direction.

4. THEORETICAL STUDY OF THE RADIATED FIELD

In the derivation of the expressions for the components of the radiated field at a distant point P due to $J_{\phi'}$ and $J_{r'}$, it will be convenient to assume that $J_{\phi'}$ and $J_{r'}$ vary as exp $(j\phi')$ and in the final expressions the real or imaginary parts may be taken as the case may be.

The distance r'' (Fig. 1) of the distant point $P(r, \theta, \phi)$ from a typical surface current element $d\Sigma$ on the conical surface (iii) situated at a point (r', θ', ϕ') is given by

$$\begin{aligned} r'' &= r - r' \cos \theta_1 \cos \theta - r' \sin \theta_1 \sin \theta \cos (\phi - \phi') \\ &= r - z \cos \theta - \rho \sin \theta \cos (\phi - \phi') \end{aligned} \tag{13}$$

where

$$d\Sigma = r' \sin \theta d\phi' \, dr'.$$

Using Schelkunoff's Equivalence Principle, the magnetic and electric vector potential $\vec{A}$ and $\vec{F}$ at the distant point P are given by

$$\vec{A} = \frac{1}{4\pi} \int_{\Sigma} \frac{\vec{J} \exp(-jk_0 r'')}{r''} \, d\Sigma \tag{14}$$

$$\vec{F} = \frac{1}{4\pi} \int_{\Sigma} \frac{\vec{M} \exp(-jk_0 r'')}{r''} \, d\Sigma \tag{15}$$

where $\vec{J}$ and $\vec{M}$ are the surface currents on surface Σ. Figure 5 shows the surface Σ which consists of surfaces (i), (iii) and the outer surface of cylindrical conducting waveguide together with a very large sphere. Only the components $J_{\phi'}$ and $J_{r'}$ of the surface electric current on surface (iii) are

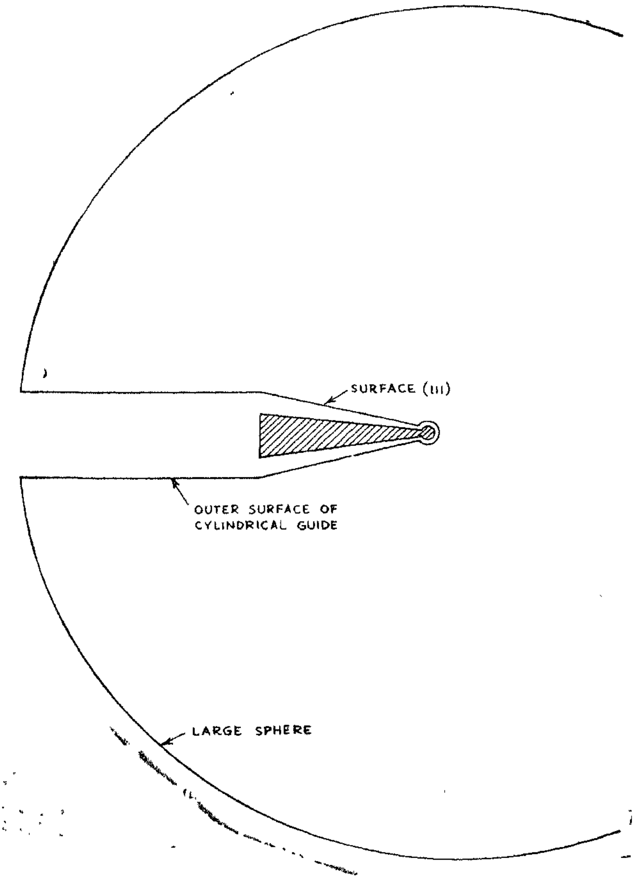

FIG. 5. Surface Σ used in the application of Schelkunoff's equivalence principle.

predominant, while the magnetic currents are negligible. Since surface (i) is very small compared to surface (iii), the contribution of the surface currents on (i) is negligible. The contribution of the surface currents on the rest of the surface Σ may be neglected.

Due to the surface current $J_{\phi'}$ on surface (iii) as given by equation (11), the x and y components of the magnetic vector potential $\vec{A}_1$ at the distant point P are given by

$$
\begin{aligned}
A_{x_1} &= K_1 \exp(j\omega t) \int_{\phi'=0}^{2\pi} \int_{r'=a}^{r_0} \frac{\exp(-jk_0 r'')}{r''} \\
&\quad \times \left[\frac{\exp(jk_2 r') + R\exp(-jk_2 r')}{k_2 r'}\right] \\
&\quad \times \exp(j\phi')(\sin\phi')\, r' \sin\theta_1\, d\phi'\, dr' \\
&= \frac{-K_1 \exp\{j(\omega t - k_0 r)\}\sin\theta_1}{k_2 r} \\
&\quad \times \int_{r'=a}^{r_0} 2\pi j\, [J_2(k_0 r' \sin\theta_1 \sin\theta)\exp(j2\phi) \\
&\quad + J_0(k_0 r' \sin\theta_1\sin\theta)]\left[\exp\left\{(jk_0 r')\left(\frac{k_2}{k_0} + \cos\theta_1\cos\theta\right)\right\}\right. \\
&\quad \left. + R\exp\left\{(-jk_0 r')\left(\frac{k_2}{k_0} - \cos\theta_1\cos\theta\right)\right\}\right] dr' \qquad (16)
\end{aligned}
$$

$$
\begin{aligned}
A_{y_1} &= K_1 \exp(j\omega t) \int_{\phi'=0}^{2\pi} \int_{r'=a}^{r_0} \frac{\exp(-jk_0 r'')}{r''} \\
&\quad \times \left[\frac{\exp(jk_2 r') + R\exp(-jk_2 r')}{k_2 r'}\right] \\
&\quad \times \exp(j\phi')(\cos\phi')\, r' \sin\theta_1\, d\phi'\, dr' \\
&= \frac{K_1 \exp\{j(\omega t - k_0 r)\}\sin\theta_1}{k_2 r} \\
&\quad \times \int_{r'=a}^{r_0} 2\pi\, [-\exp(2j\phi) J_2(k_0 r' \sin\theta_1 \sin\theta) \\
&\quad + J_0(k_0 r' \sin\theta_1\sin\theta)]\left[\exp\left\{(jk_0 r')\left(\frac{k_2}{k_0} + \cos\theta_1\cos\theta\right)\right\}\right. \\
&\quad \left. + R\exp\left\{(-jk_0 r')\left(\frac{k_2}{k_0} - \cos\theta_1\cos\theta\right)\right\}\right] dr' \qquad (17)
\end{aligned}
$$

where

$$k_0 = \frac{2\pi}{\lambda_0} = \omega\sqrt{\mu_0\epsilon_0},\ \lambda_0 \text{ being the free-space wavelength}$$

$$k_2 = \frac{2\pi}{\lambda_g},\ \lambda_g \text{ being the measured guide wavelength}$$

r_0 = finite length of the dielectric-coated spherically-tipped conducting cone antenna

a = radius of the spherical conducting tip.

The θ and ϕ components of the electric field intensity $\vec{E_1}$ at the distant point are given by

$$E_{\theta_1} = (E_{x_1} \cos\phi + E_{y_1} \sin\phi) \cos\theta \tag{18}$$

$$E = (-E_{x_1} \sin\phi + E_{y_1} \cos\phi) \tag{19}$$

where

$$E_{x_1} = -j\omega\mu A_{x_1}$$
$$E_{y1} = -j\omega\mu A_{y_1}. \tag{20}$$

Because $|J_{\phi'}| = |H_{r'}| \propto \cos\phi' = Re \exp(j\phi')$, taking the real parts of the final expressions, E_{θ_1} and E_ϕ, are given by

$$E_{\theta_1} = \frac{K_1' \exp\{j(\omega t - k_0 r)\} \sin\theta_1}{r}$$
$$\times \int_{r'=0}^{r_0} \cos\theta\,[J_0(k_0 r' \sin\theta_1 \sin\theta)\sin\phi$$
$$-\sin(3\phi)\,J_2(k_0 r' \sin\theta_1 \sin\theta)]$$
$$\times \left[\exp\left\{(jk_0 r')\left(\frac{k_2}{k_0} + \cos\theta_1\cos\theta\right)\right\}\right.$$
$$\left.+ R\exp\left\{(-jk_0 r')\left(\frac{k_2}{k_0} - \cos\theta_1\cos\theta\right)\right\}\right] dr^1 \tag{21}$$

$$E_{\phi_1} = \frac{K_1' \exp\{j(\omega t - k_0 r)\} \sin\theta_1}{r}$$
$$\times \int_{r'=a}^{r_0} [J_0(k_0 r' \sin\theta_1 \sin\theta)\cos\theta$$
$$-\cos(3\phi)\,J_2(k_0 r' \sin\theta_1 \sin\theta)]$$
$$\times \left[\exp\left\{(jk_0 r')\left(\frac{k_2}{k_0} + \cos\theta_1\cos\theta\right)\right\}\right.$$
$$\left.+ R\exp\left\{(-jk_0 r')\left(\frac{k_2}{k_0} - \cos\theta_1\cos\theta\right)\right\}\right] dr' \tag{22}$$

where

$$K_1^1 = \frac{-j\omega\mu 2\pi K_1}{k_2}. \tag{23}$$

Now, considering the component J_{r_1} of the surface electric current density on surface (iii), $|J_{r'}| = |H_{\phi'}|$ and $|H_{\phi'}| \propto \sin\phi' = Im \exp(j\phi')$. At diametrically opposite points A and A' on the circle which is a cross-section of the conical surface (iii) $\theta = \theta_1$ (*see* Fig. 1), $J_{r'}$ is equal in magnitude but opposite in direction. Because of this fact, the components $J_{r'}$ at these diametrically opposite points subtract in the z direction but add in the ρ direction in the x-y plane. Hence it is necessary to consider only the contribution of the ρ component $J_{r'} \sin\theta_1$ of $J_{r'}$ in calculating the far field.

The components E_{θ_2} and E_{ϕ_2} of the electric field intensity $\vec{E}_2$ due to $J_{r'}$ at the distant point P are then given by

$$E_{\theta_2} = \frac{K_2'}{r} \exp\{j(\omega t - k_0 r)\} \sin^2\theta_1 \int_{r'=a}^{r_0} \cos\theta \\ [-\sin(3\phi) J_2(k_0 r' \sin\theta_1 \sin\theta) - \sin\phi\, J_0(k_0 r' \sin\theta_1 \sin\theta)] \\ \left[\exp\left\{(jk_0 r')\left(\frac{k_2}{k_0} + \cos\theta_1 \cos\theta\right)\right\} + R\exp\left\{(-jk_0 r') \right.\right. \\ \left.\left. \times \left(\frac{k_2}{k_0} - \cos\theta_1\cos\theta\right)\right\}\right] dr' \tag{24}$$

and

$$E_{\phi_2} = \frac{K_2' \exp\{j(\omega t - k_0 r)\} \sin^2\theta_1}{r} \int_{r'=a}^{r_0} \\ \times [-\cos(3\phi) J_2(k_0 r' \sin\theta_1 \sin\theta) - \cos\phi\, J_0(k_0 r' \sin\theta_1 \sin\theta)] \\ \times \left[\exp\left\{(jk_0 r')\left(\frac{k_2}{k_0} + \cos\theta_1\cos\theta\right)\right\} + R\exp\left\{(-jk_0 r')\left(\frac{k_2}{k_0}\right.\right.\right. \\ \left.\left.\left. - \cos\theta_1\cos\theta\right)\right\}\right] dr' \tag{25}$$

where

$$K_2^1 = -j\omega\mu 2\pi K_2. \tag{26}$$

The total electric field intensity E has θ and ϕ components given by

$$E_\theta = E_{\theta_1} + E_{\theta_2} \tag{27}$$

and

$$E_\phi = E^{\phi}{}_1 + E_{\phi_2}.$$

5. Radiation Patterns in the Principal $\phi = 0^0$ and $\pi = 90^0$ Planes

In $\phi = 0^0$ *Plane*,

$$E_{\theta_1} = E_{\theta_2} = 0$$

Hence the normalized radiation power pattern is given by

$$\left| \frac{E}{E_{\max}} \right|^2 = \frac{|f_2(\theta)|^2}{|f_2(\theta)|^2_{\max}} \tag{28}$$

where

$$f_2(\theta) = \sin\theta_1 \int_{r'=a}^{r_0} [J_0(k_0 r' \sin\theta_1 \sin\theta) - J_2(k_0 r' \sin\theta_1 \sin\theta)]\left[\exp\left\{(jk_0 r'\left(\frac{k_2}{k_0} + \cos\theta_1\cos\theta\right)\right\} + R\exp\left\{(-jk_0 r')\left(\frac{k_2}{k_0} - \cos\theta_1\cos\theta\right)\right\} dr' \tag{29}$$

In $\phi = 90^0$ *Plane*,

$$E_{\phi_1} = E_{\phi_2} = 0.$$

Hence the normalized radiation power pattern is gven by

$$\frac{|E|^2}{|E_{\max}|^2} = \frac{|f_1(\theta)|^2}{|f_1(\theta)|^2_{\max}} \tag{30}$$

where $f_1(\theta)$ is given by

$$f_1(\theta) = \sin\theta_1 \int_{r'=a}^{r_0} [J_0(k_0 r' \sin\theta_1 \sin\theta) + J_2(k_0 r' \sin\theta_1 \sin\theta)] \times \left[\exp(jk_0 r')\left(\frac{k_2}{k_0} + \cos\theta_1\cos\theta\right) + R\exp(-jk_0 r') \times \left(\frac{k_2}{k_0} + \cos\theta_1\cos\theta\right)\right] \mathrm{d}r'. \tag{31}$$

6. Total Power Radiated and Directive Gain

The total power radiated is

$$W = \int_{\phi=0}^{2\pi} \int_{\theta=0}^{\pi} \frac{(E_\theta^2 + E_\phi^2)}{\eta} r^2 \sin\theta \, d\theta d\phi \tag{32}$$

where

$$\eta^2 = \frac{\mu_0}{\epsilon_0}$$

and the directive gain of the antenna is given by

$$G = \frac{4\pi\, [r^2 (E_\theta{}^2 + E_\phi{}^2)]_{max}}{\eta W.} \tag{33}$$

The final expressions for W and G are given by

$$W = \frac{C_1{}^2}{r^2} \frac{\pi}{\eta} \int_{\theta=0}^{\pi} [\{ | f_3 (\theta) | \}^2 + \{ | f_4 (\theta) | \}^2]$$

$$(1 + \cos^2 \theta) \sin \theta \, d\theta \tag{34}$$

and

$$G = \frac{4\ [| f_2 (\theta) |]^2_{max\ at\ \theta=0}}{\int_{\theta=0}^{\pi} \{| f_3 (\theta) |^2 + | f_4 (\theta) |^2\} (1 + \cos^2 \theta) \sin d\theta} \tag{35}$$

where

$$f_3 (\theta) = \sin \theta_1 \int_{r_1=a}^{r_0} [J_0 (k_0 r' \sin \theta_1 \sin \theta)]$$

$$\times \left[\exp\left\{(jk_0 r') \left(\frac{k_2}{k_0} + \cos \theta_1 \cos \theta\right)\right.\right.$$

$$\left.\left. + R \exp \left\{(- jk_0 r') \left(\frac{k_2}{k_0} + \cos \theta_1 \cos \theta\right)\right\}\right] dr' \tag{36}$$

and

$$f_4 (\theta) = \sin \theta_1 \int_{r^1=a}^{r_0} [J_0 (k_0 r' \sin \theta_1 \sin \theta)]$$

$$\times \left[\exp \left\{(jk_0 r') \left(\frac{k_2}{k_0} + \cos \theta_1 \cos \theta\right)\right\}\right.$$

$$\left. + R \exp \left\{(- jk_0 r') \left(\frac{k_2}{k_0} - \cos \theta_1 \cos \theta\right)\right\}\right] dr' \tag{37}$$

7. NUMERICAL COMPUTATIONS OF THE RADIATION PATTERNS AND DIRECTIVE GAIN

The radiation patterns in the $\phi = 0°$ and $\pi = 90°$ planes and the gain have been numerically computed for several antennas of varying dimensions using equations (28), (30) and (35). The results are given in Figs. 6 to 12 together with the experimental curves.

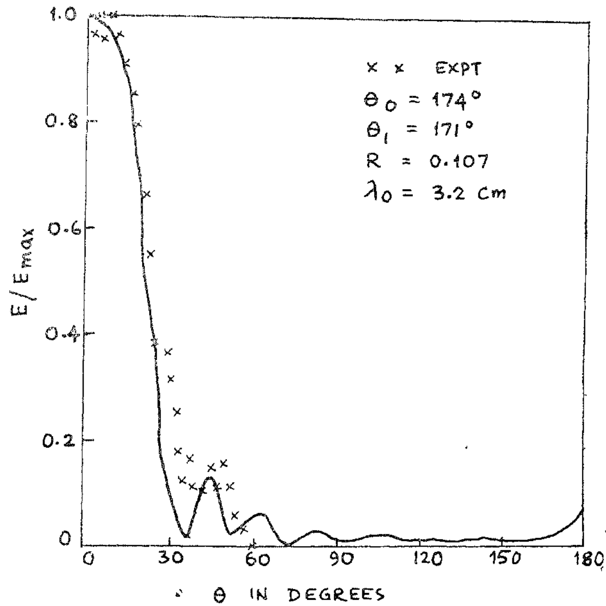

FIG. 6. Calculated and measured H- plane radiation pattern of the dielectric coated metal cone antenna.

8. Experimental Investigations

The following experimental investigations on the antennas have been carried out as a function of the length and taper angles:

(*a*) Study of the near field components of the electric and magnetic field.

(*b*) Study of the radiation patterns.

(*c*) Measurement of the gain of the antennas by the (i) reflection [15] and (ii) comparison methods.

(*d*) Study of the impedance trransforming characteristics of the mode transducer used to launch the HE mode on the antenna by measurement of scattering coefficients [16].

(*e*) Study of the input impedance of the antennas.

Some of the results of the experimental investigations are given in Figs. 6 to 15.

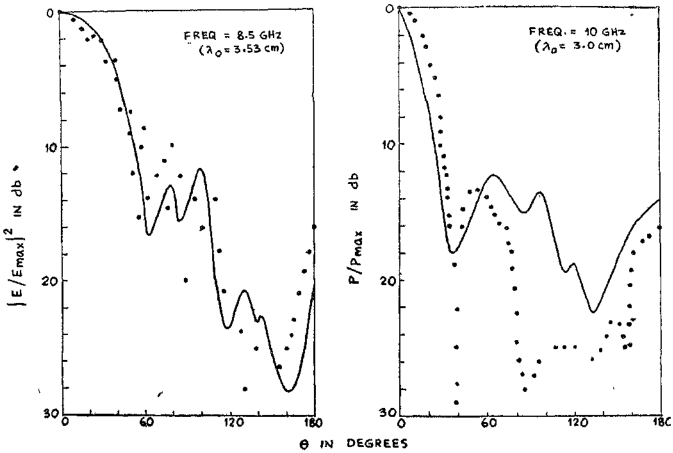

FIG. 7.

.... EXPERIMENTAL
—— THEORETICAL

9. DISCUSSION OF THE THEORETICAL AND EXPERIMENTAL RESULTS

(*a*) *Near Field*

The near field measurements made on a number of antennas to study the variation of the field components verify

(i) the assumption that the field components vary as cos ϕ' (Fig. 2)

(ii) the assumptions given by equations (11) and (12) is approximately correct (Figs. 3 and 4).

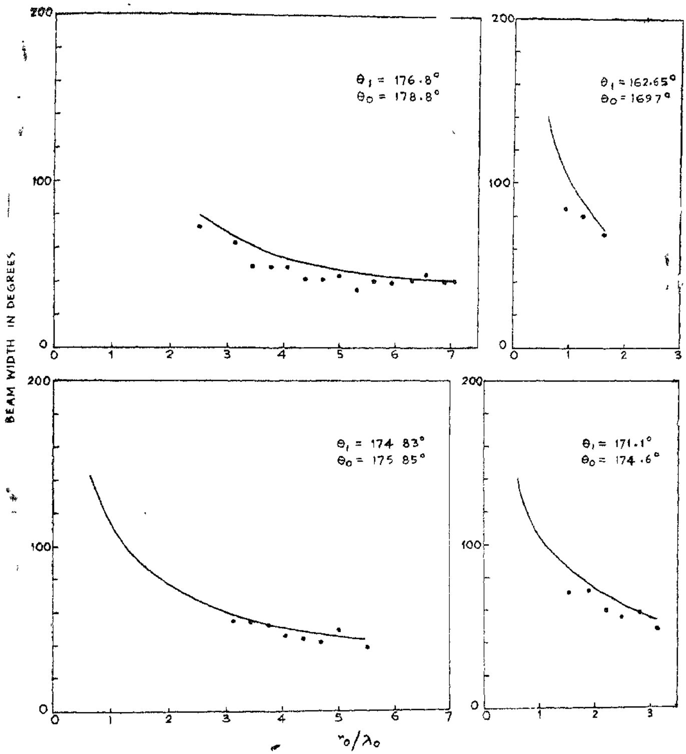

FIG. 8. Calculated and observed beam widths of the major lobe
—— Calculated, ... Experimental.

(iii) The hybrid HE mode is excited (as shown by the existence of all the field components $E_{r'}$, $E_{\theta'}$, $E_{\phi'}$, $H_{r'}$, $H_{\theta'}$, $H_{\phi'}$.

(*b*) *Radiation Patterns*

Figures 6 to 12 show the theoretical and experimental results of the radiation patterns. It may be observed that:

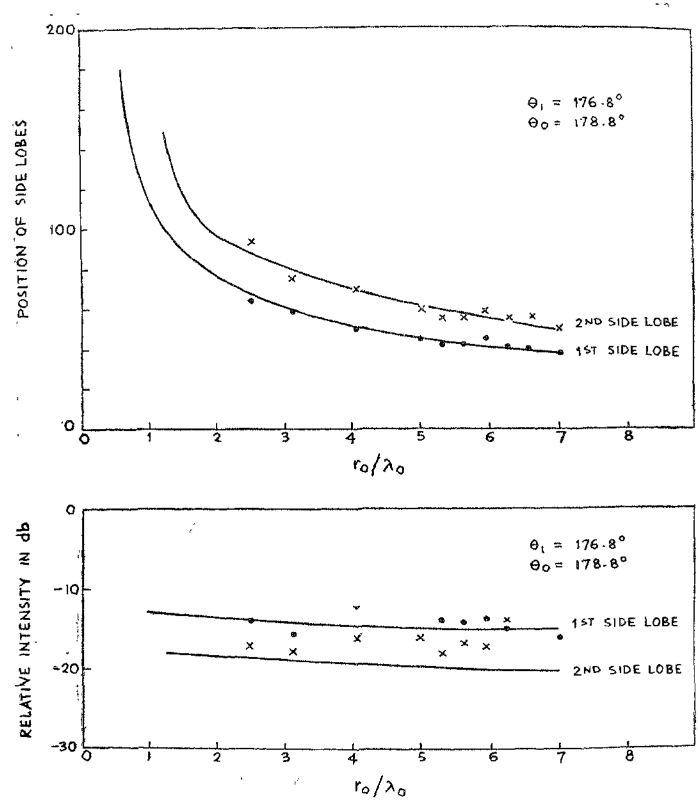

FIG. 9. Calculated and observed positions and relative intensities of the side lobes. —— Calculated, ... Observed 1st lobe, × × Observed 2nd lobe.

(i) The positions of the major lobe and the first two side lobes which could be experimentally observed agree fairly well with theory.

(ii) There is fair agreement between the theoretical and experimental beam widths and positions of the nulls.

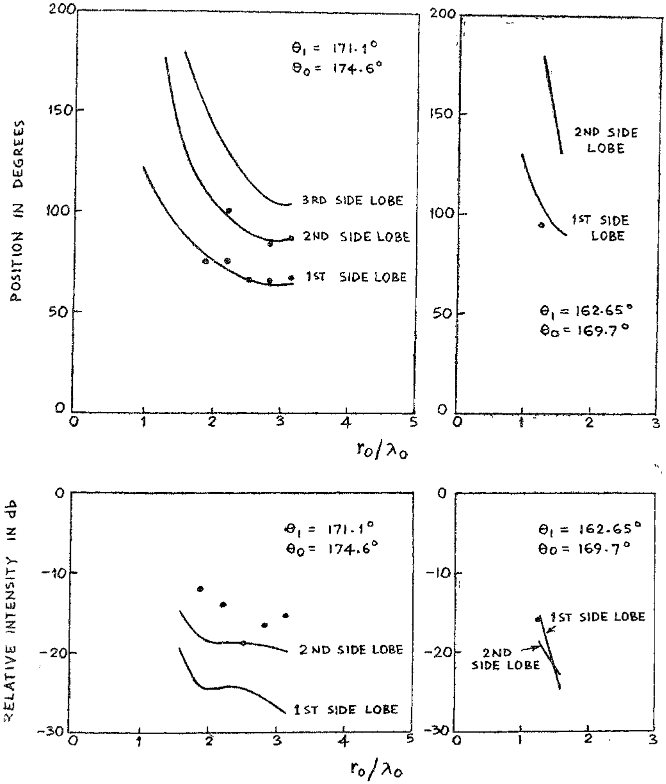

FIG. 10. Calculated and observed positions and relative intensities of the side lobes. —— Calculated, ... Observed.

(iii) The first side lobe is 14 to 20 dbs and the second side lobe is 20 to 30 dbs below the major lobe, while the higher order side lobes are more than 25 db below the major lobe. It may therefore be said that this type of antenna yields a strong axial major lobe and well suppressed side lobes,

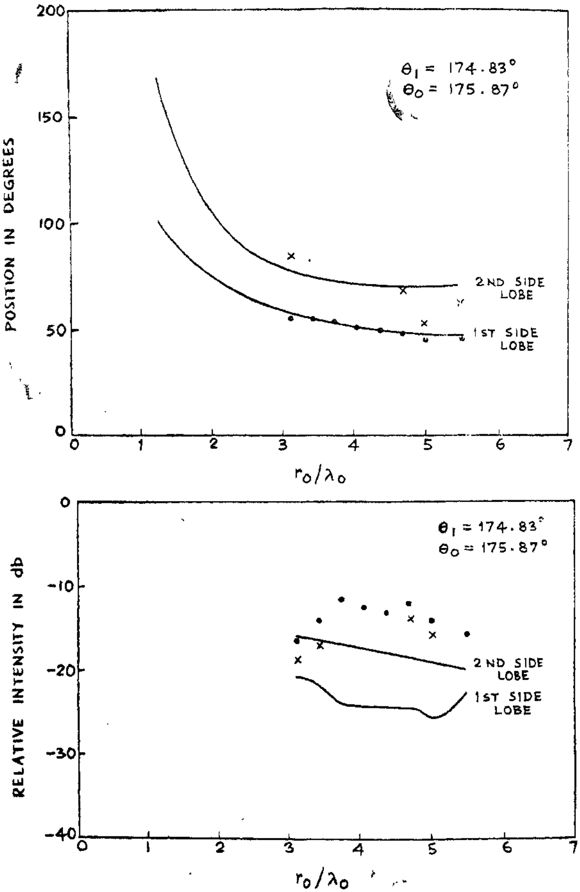

FIG. 11. Calculated and observed positions and relative intensities of the side lobes.
—— Calculated, ... Observed 1st lobe, × × Observed 2nd lobe.

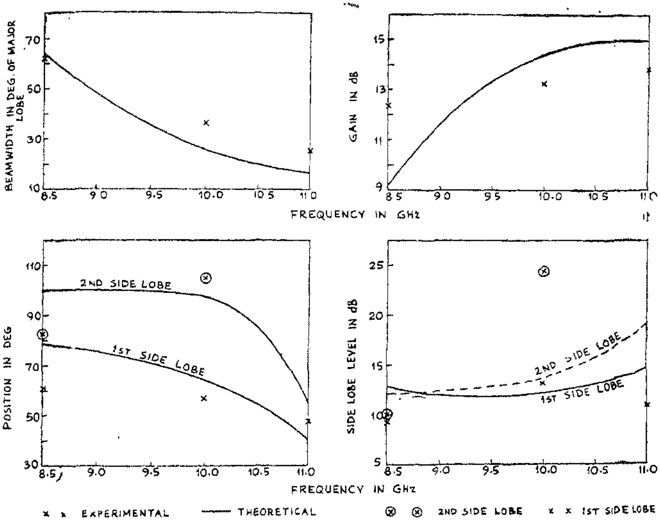

FIG. 12

(c) Gain

Figures 13 and 14 show the calculated and experimental values of the gains of the antennas. It may be observed that:

(i) For longer antennas the theoretical gain agrees with the experimental values obtained by both methods.

(ii) For shorter antennas the theoretical gain agrees better with the experimental value obtained by the comparison method than by the reflection method. This is possibly due to the fact that due to high reflection coefficient the reflection method cannot be expected to give correct results.

(*d*) Figures 15 and 16 show a plot of the impedance characteristics of the antenna as a function of length. The almost constant input impedance characteristics of the antenna having different taper angles and different lengths shows that the antenna possesses broad-band characteristics.

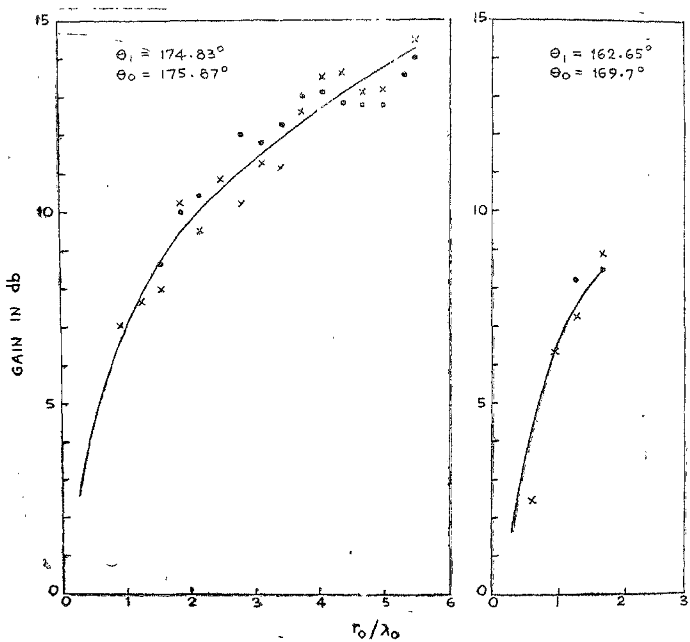

FIG. 13. Calculated and observed gain of the aerials.

—— Theoretical

.... Experimental (Reflection method)

× × Experimental (Comparison method)

10. CONCLUSIONS

As a result of the theoretical and experimental investigations on the dielectric-coated spherically-tipped conducting cone antennas it may be concluded that:

(i) The antenna excited in the unsymmetric hybrid mode behaves like an end fire antenna having a narrow major lobe and a large number of minor lobes of very low intensities.

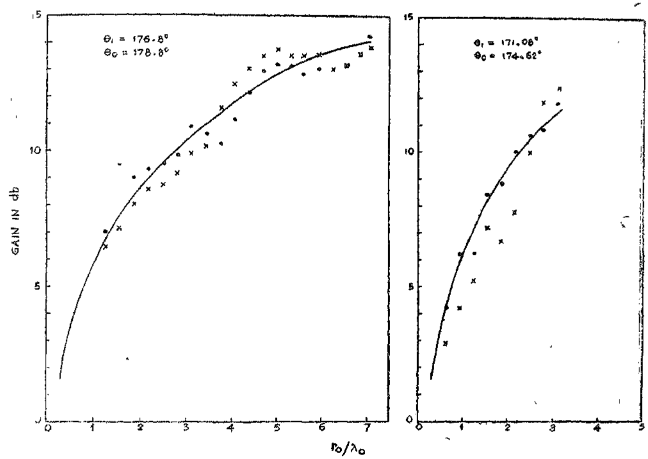

FIG. 14. Calculated and observed gain of the arials.

—— Theoretical

• • • • Experimental (Reflection method)

× × Experimental (Comparison method)

(ii) The beam width of the major lobe can be minimized and the gain of the antennas maximized by proper choice of the angles θ_0 and θ_1 of the cones for a given length r_0 of the antenna.

(iii) The antenna has broad-band characteristics as shown by the radiation and impedance characteristics.

More details of the work are contained in [17].

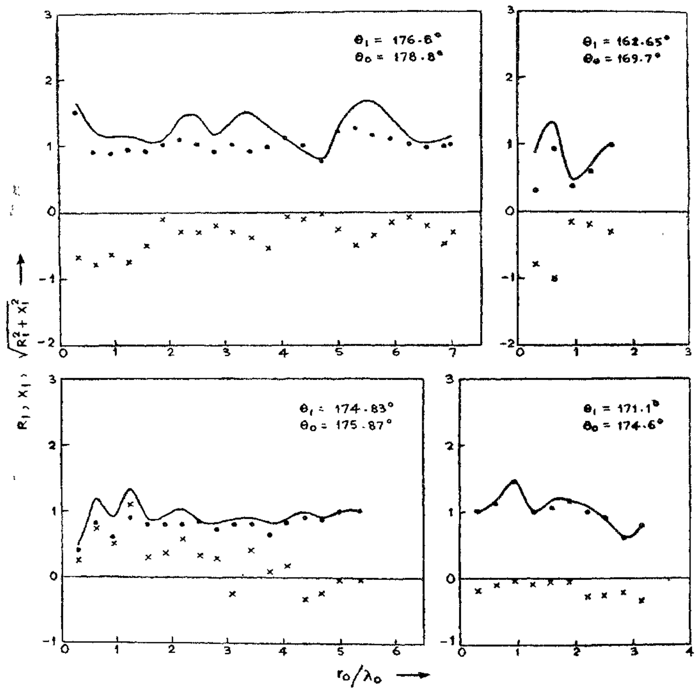

Fig 15 Variation of relative input impedance $\sqrt{R_1^2 + X_1^2}$, the resistive part R_1 and the reactive part X_1

—— $\sqrt{R_1^2 + X_1^2}$, • • Resistive part R_1, × × Reactive part X_1

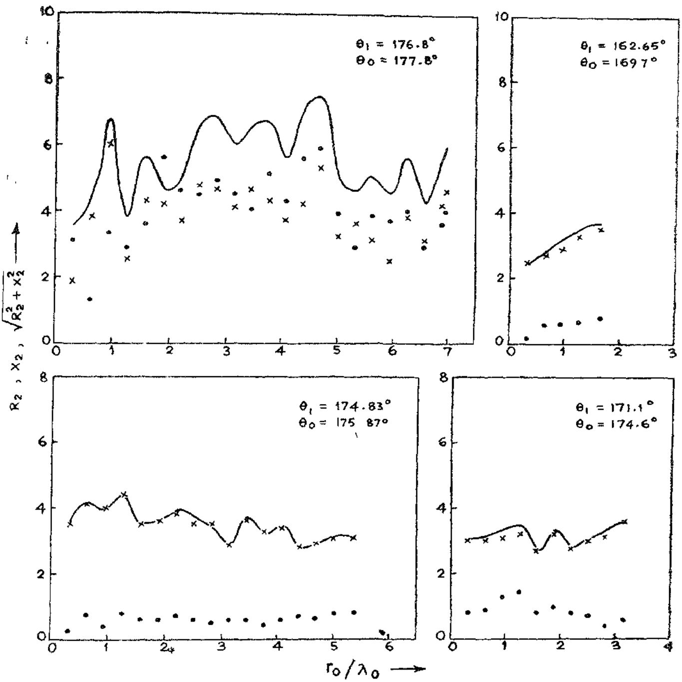

Fig 16 Variation of relative input impedance $\sqrt{R_2^2+X_2^2}$, the resistive part R_2 and the reactive part X_2

—— $\sqrt{R_2^2+X_2^2}$, • • Resistive part R_2, × × Reactive part X_2

ACKNOWLEDGEMENTS

The authors wish to express their gratitude to Dr. S. Dhawan, Director of the Indian Institite of Science, Bangalore, for providing facilities for carrying out the investigations. They are also grateful to the Council of Scientific and Industrial Research for the sanction of a research scheme on the above subject.

REFERENCES

[1] Schorr, M. G. and Beck, F. J. Electromagnetic Field of a conical horn, *Journ. Appl. Phys.*, 1950, **21**, 795.

[2] Felsen, L. B. .. Backscattering from wide-angle and Narrow-angle cones, *Journ. Appl. Phys.*, 1955, **26**, 138.

[3] Felsen, L B. .. Alternative field representations in regions bounded by spheres, Cones and planes, *I. R. E. Trans.*, 1957, Vol AP-5, p. 109.

[4] Felsen, L. B. .. Plane-wave scattering by small-angle cones, *I.R.E. Trans.*, Vol. AP-5, p. 121.

[5] Felsen, L. B. .. Radiation from ring sources in the presence of a semi-infinite cone, *I.E.E.E. Trans.*, 1959, Vol. AP-7, p. 168.

[6] Felsen, L. B. .. Electromagnetic properties of wedge and cone surfaces with a linearly varying surface impedance, *I.E.E.E. Trans.*, 1959, Vol. AP-7, Sp. Suppl., p. S231.

[7] Felsen, L. B. .. Radiation from tapered surface wave antenna, *I.E.E.E. Trans.*, 1960, Vol. AP-8, p. 577.

[8] Adachi, S. .. A theoretical analysis of semi-infiinte conical antenna, *I.E.E.E. Trans.* 1960, Vol. AP-8, p. 534.

[9] Adachi, S., Kouyoumjian, R. G. and Van Sickle, R. G. The finite conical antenna, *I.E.E.E. Trans.*, 1959, Vol. AP-7 Sp. Suppl., p. S406.

[10] Wait, J. R. .. *Electromagnetic Radiation from Conical Structures*. Chap, 12, pp. 483, *Antenna Theory*, Part I, Edited by R. E. Collin and F. J. Zucker, Mcgraw-Hill Book Co., N.Y.

[11] Yeh, C. .. An application of sommerfeld's complex order wave. functions to an antenna problem, *Journ. Math. Phys.*, 1964, **5** (3), 344.

[12] Chatterjee, R. .. Radiation from a dielectric-coated, spherically-tripped perfectly conducting cone, *Journ. Ind. Inst. Sci.*, 1970, **52** (1), 48.

[13] Chatterjee, R. and Vedavathy, T. S. Dielectric-coated spherically-tipped metal cone antennas excited in unsymmetric mode at microwave frequencies, *Journ. Asia Electronics Union*, No. 2, Serial No, 16, 1972, pp. 45-49.

[14] Chatterjee, R. and Vedavathy, T. S. Dielectric-coated spherically-tipped metal cone antennas excited in unsymmetric hybrid mode at microwave frequencies, 2-11 D3, *Proc. International Symposium on Antennas and Propagation* held at Tohoku University, Sendai, Japan, September. 1-3, 1971.

[15] Barlow, H. M. and Cullen, A. L. *Microwave Measurements*, Constable and Co., Ltd., London.

[16] Deschamps, G. A. .. Determination of reflection coefficient and insertion loss of a waveguide junction, *Journ. Appl. Phys.*, 1953. 24, (8), pp. 1006.

[17] Vedavathy, T. S. .. *Dielctric-coated Spherically-tipped Metal Cone Aerials Exeited in the Unsymmetric Hybrid Mode*, A thesis submitted for the Ph.D. degree of the Indian Institite of Science, Bangalore, India, 1972.

Calendar of events: Conferences/Symposia at the Indian Institute of Science Campus

Sl. No.	Name of the School	Period	Sponsoring Department of the Institute
1.	Lecture Course on Cavitation	November to December 1975	Chemical Engineering
2.	QIP—" Organization and Logical Design	24th November to 6 December 1975	School of Automation
3.	Crystal Chemistry for College Teachers	December 1975	Inorganic and Physical Chemistry
4.	QIP—" Wind Tunnel Technique "	15–27 December 1975	Aeronautical Engineerin
5.	5th Asian Regional Conference on Soil Mechanics and Foundation Engineering	18–22 December 1975	Civil Engineering
6.	QIP—for Teachers in Engineering Colleges	16–31 December 1975	Chemical Engineering
7.	QIP—Design and Performance Estimation of Heat Exchangers	1–14 February 1976	Mechanical Engineering
8.	" Design and Technology of Digital Equipment "	9–21 February 1976	Electrical Communicatio Engineering
9.	" Dynamics and Control of Industrial Organisers "	12–25 February 1976	Chemical Engineering
10.	"QIP—Public Water Supply/Systems "	16–29 February 1976	Chemical Engineering
11.	QIP—" Dynamics of Engineering Systems "	1–15 March 1976	School of Automation and Mechanical Engineering

On the basis of the information received by the Editorial Office on 30th October 1975.